Acta Cryst. (1975). B31, 1998

The Crystal Structure of Deuterium Fluoride

BY M. W. JOHNSON,* E. SÁNDOR AND E. ARZI

Queen Mary College, Mile End Road, London E1 4NS, England

(*Received* 6 *September* 1974; *accepted* 24 *February* 1975)

The crystal structure of DF (at 4·2 K and 85 K) has been determined by the neutron powder diffraction method. The structure is orthorhombic ($Bm2_1b$: No. 36, standard symbol $Cmc2_1$–C_{2v}^{12}) with $a=3{\cdot}31$ (1), $b=4{\cdot}26$ (1), $c=5{\cdot}22$ (1) at 4·2 K and $a=3{\cdot}33$ (1), $b=4{\cdot}27$ (1), $c=5{\cdot}27$ (1) Å at 85 K. There are four DF molecules in the unit cell forming zigzag chains parallel to the b axis. Neighbouring chains are parallel, resulting in a polar structure. F–F–F angle 116° (1), F–F distance 2·50 (1) at 4·2 K, 2·51 (2) Å at 85 K. The intramolecular bond length is 0·97 (2) at 4·2 K, 0·95 (3) Å at 85 K and the length of the hydrogen bond is 1·53 (2) at 4·2 K, 1·56 (3) Å at 85 K. Final R values (intensities): 0·069 (isotropic, 85 K), 0·049 anisotropic, 4·2 K).

Introduction

Although there have been few reported experiments on solid DF, there have been many on its expected isomorph solid HF. The specific-heat curve for HF (see Clusius, Hiller & Vaughan, 1930; Dahmlos & Jung, 1933; Hu, White & Johnston, 1953) shows no sign of any phase transition in the solid state. This is to be expected from the strong hydrogen bonding which is responsible for molecular-chain formation even in the liquid and gas phases (Briegleb, 1941, 1942, 1943; Smith, 1958; Ring & Egelstaff, 1969, 1970).

X-ray and electron-diffraction studies of solid HF (Bauer, Beach & Simons, 1939; Günther, Holm & Strunz, 1939; Atoji & Lipscomb, 1954) have shown that the fluorine atoms form a face-centred orthorhombic lattice ($Bmmb$–D_{2h}^{17}) with unit-cell parameters $a=3{\cdot}42$, $b=4{\cdot}32$, $c=5{\cdot}41$ Å at 148 K. Although these studies did not allow an unambiguous determination of the position of the hydrogen atoms, the structure of solid HF was thought to be one of those shown in Fig. 1: (i) a parallel-chain model [Fig. 1(*a*), $Bm2_1b$], (ii) an anti-parallel chain model [Fig. 1(*b*), *Pmnb*], or (iii) a disordered model in which the hydrogen atoms occupy either of two equally probable positions [Fig. 1(*c*), *Bmmb*].†

Subsequent infrared, Raman and inelastic neutron-scattering experiments (Boutin, Safford & Brajovic, 1963; Giguère & Zengin, 1958; Kittelberger & Hornig, 1967; Sastri & Hornig, 1963) have not settled the question of the hydrogen position in solid HF either, although Kittelberger & Horning (1967) suggest that their infrared and Raman data indicate a disordered structure (*Bmmb*).

Recent n.m.r. measurements (Habuda & Gagarinsky, 1971, 1972) have given estimates of the intramolecular bond length in solid HF, and the authors have concluded that the structure should be the anti-parallel one [Fig. 1(*b*), *Pmnb*]. In addition a SCFMO calculation (Bacon & Santry, 1972) of the binding energies of the parallel and antiparallel chain models has suggested that the antiparallel structure is more stable by 2 kcal mole^{-1}.

The present investigation was carried out in order to test these contradictory proposals.

Experiment

DF was prepared by the reduction of AgF_2 by deuterium at ~120 °C (Herber, 1962)

$$AgF_2 + D_2 \rightarrow Ag + 2DF\,.$$

When the reaction was completed, the copper reaction vessel (~300 c.c.) was opened to a stainless-steel storage tube, the end of which was kept at 77 K. This enabled the DF to be condensed out of the system, leaving behind any residual deuterium gas. The AgF_2 (99·9%) was obtained from the Johnson and Matheson Co. and the deuterium gas from the electrolysis of D_2O (99·9%) acidified with a small quantity of D_2SO_4 (both supplied by the Koch Light Co.).

Because of its chemical reactivity, the sample was stored in a stainless-steel tube kept in liquid nitrogen. At the beginning of each neutron-diffraction experiment the sample was transferred from the stainless-steel storage tube into a KEL-F (trifluoromonochloropolyethylene, obtained from the Flurocarbon Co.) tube ($\varphi=10$ mm), by sublimation. The receiving KEL-F tube was kept at 77 K by liquid nitrogen. During the transfer the DF gas was only allowed to come into contact with either stainless steel, Teflon or KEL-F. Considerable care was taken to obtain good

* Present address: Computer & Automation Division, Building R1, Rutherford Laboratory, Chilton, Didcot, Oxon OX11 0QX, England.

† The non-standard space-group symbols which have been used throughout have the following corresponding symbols. $Bm2_1b$: No. 36, standard symbol $Cmc2_1$–C_{2v}^{12}; *Pmnb*: No. 62, standard symbol *Pnma*–D_{2h}^{16}; *Bmmb*: No. 63, standard symbol *Cmcm*–D_{2h}^{17}.

powder samples, and a number of powder samples were rejected because of preferred orientation.

Neutron powder diffraction patterns were recorded using the Curran and Panda instruments at the research reactors DIDO and PLUTO at AERE, Harwell. The number of observed powder peaks was rather small and several of them appeared to be overlapping multiplets. In order to extract the maximum amount of information from the powder sample, the neutron diffraction pattern was recorded with three different neutron wavelengths (1·06, 1·52 and 1·89 Å). The shortest wavelength was used to record as many peaks as possible, and the longer wavelengths to separate the components of the multiplets. Details of the six diffraction experiments performed are summarized in Table 1.

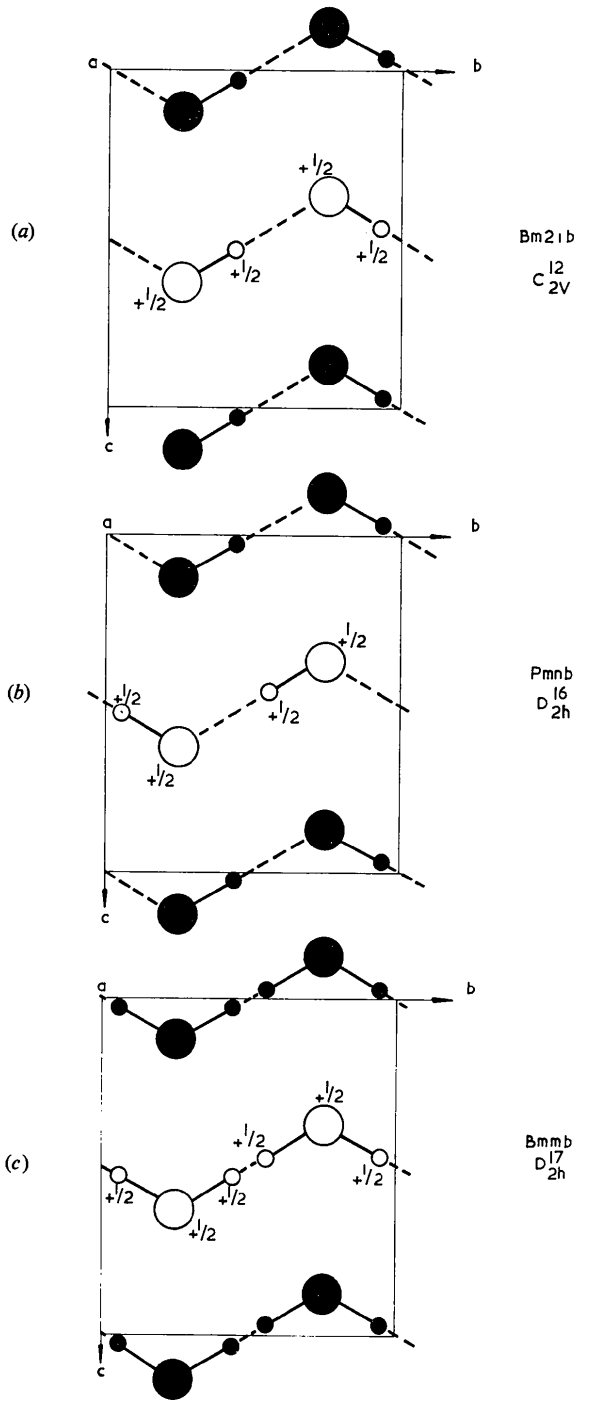

Fig. 1. Models proposed for the crystal structure of solid HF: (*a*) parallel zigzag chain model, (*b*) antiparallel zigzag chain model, (*c*) disordered zigzag chain model. The large circles represent fluorine atoms, the small circles deuterium atoms. The full circles are atoms at $a=0$, the empty circles atoms at $a=\frac{1}{2}$. The *a* axis is pointing into the page.

Table 1. *Summary of the neutron powder-diffraction patterns recorded with solid* DF

Expt	λ (Å)	T (K)	Angular range in 2θ(°)	Number of independent detectors
1	1·06	85	0–60	5
2	1·06	4·2	0–60	5
3	1·06	85	0–60	5
4	1·06	4·2	0–60	5
5	1·52	4·2	67–105	1
6	1·89	4·2	37–94	1

Since the Curran instrument had five independent detectors and θ–2θ scans were employed, experiments 1–4 furnished 20 independent sets of data. Thus there were altogether 12 independent sets of $I(hkl)$ values available for DF at 4·2K and 10 sets for DF at 85K.

All observed neutron powder peaks could be indexed on the basis of an orthorhombic unit cell similar to the one proposed by Atoji & Lipscomb (1954) for the fluorine lattice in solid HF. The values of the lattice parameters were obtained by minimizing the quantity

$$S=\sum (\theta_{\rm obs}-\theta_{\rm calc}+D)^2 \qquad (1)$$

where the parameters to be varied were *a*, *b*, *c* and *D*. Since neutron spectroscopy only allows the measurement of peaks on one side of the incident beam the absolute values of $\theta_{\rm obs}$ are not known and the parameter *D* in equation (1) must be included. The values of the lattice parameters so found are as follows:

	a	*b*	*c*
4·2K	3·31(1)	4·26(1)	5·22(1)
84K	3·33(1)	4·27(1)	5·27(1)

Though the use of a profile-fitting program increased considerably the number of individual peaks which could be extracted from the powder pattern, some groups of overlapping peaks could not be resolved even with this technique. In order to utilize these peaks as well, the full-matrix least-squares refinement program used for refining the structure was modified to obtain least-squares fit to the intensities of unresolvable multiplets.

Since the different sets of $I(hkl)$ values had different scale factors, a single set of intensities was derived

from them by minimizing the following expression with respect to c_j and $I_d(hkl)$;

$$\sum_j \sum_{hkl} \frac{1}{c_j^2\sigma_{ij}^2} [(c_j I(hkl)_j - I_d(hkl)]^2 \qquad (2)$$

where j = label of a particular set of intensity values, c_j = the scale factor of the jth set, σ_{ij} = standard deviation of ith reflexion in jth set (estimated from the peak height and background), $I(hkl)_j$ = measured intensity of ith reflexion of jth set, $I_d(hkl)$ = derived set of intensities. The standard deviations associated with the derived $I_d(hkl)$ values were obtained from

$$\sigma_d^2(hkl) = \sum_j \sigma_j^2(hkl) \left(\frac{\partial I_d(hkl)}{\partial I(hkl)_j} \right)^2 . \qquad (3)$$

The $I_d(hkl)$ and $\sigma_d(hkl)$ values used in the refinement of the structural parameters are given in Table 2.

Crystal structure

Reflexions of the type hkl: $h+l=2n+1$ and $hk0$: $k=2n+1$ were systematically absent, which made the antiparallel-chain model [D_{2h}^{16}–*Pmnb*, see Fig. 1(*b*)] a very unlikely proposition. It was finally ruled out by a comparison of the observed and calculated $I(hkl)$ values. This is illustrated in Fig. 2, where the first few calculated intensities are plotted for each of the three proposed structures together with the observed intensities. This shows that, for the antiparallel chain model, an 011 peak should appear and, on the other hand, that the strong 020 and 121 peaks should be virtually absent from the diffraction pattern [*cf.* Figs. 2(*a*) and 2(*d*)].

The other two structures shown in Figs. 1(*a*) and 1(*c*) both give rise to systematic absences consistent with the observed diffraction pattern. However, the disordered model (*Bmmb*), like the antiparallel-chain model, would produce unacceptably low values for the 020 and 121 peaks [*cf.* Fig. 2(*b*) and (*d*)]. Hence, this too was eliminated.

Finally, the parallel-chain model [Fig. 1(*a*)] was not only consistent with the systematic absences but was also compatible with the observed intensities [*cf.* Fig. 2(*c*) and (*d*)]. Accordingly this model was considered to represent the correct structure and the final full-matrix least-squares refinements based on this model reached residuals (for the intensities) of 4·9% for the 4·2 K data and 6·9% for the 85 K data.

Table 2. *Comparison of the observed intensities (I_d) with the calculated ones (I_{calc}) obtained* (i) *after five cycles of anisotropic refinement (at* 4·2 K*) and* (ii) *after five cycles of isotropic refinement (at* 85 K*) respectively, together with the standard deviations of the observed values (σ_d)*

	4·2 K			85 K		
h k l	I_d	I_{calc}	σ_d	I_d	I_{calc}	σ_d
1 0 1	1102	1094	0·8	463	462	0·4
0 0 2	137·1	152·6	0·5	64·8	68·4	0·3
1 1 1	302·3	304·9	0·6	116·1	120·7	0·3
0 1 2	288·6	306·9	0·6	127·5	120·8	0·3
0 2 0	77·5	55·0	0·5	44·3	30·1	0·3
1 2 1	112·7	120·7	0·5	52·1	55·1	0·3
2 0 0	380·6	354·1	0·9	76·7	89·8	0·3
0 2 2				40·5	40·0	0·3
1 1 3	205·8	184·2	0·6	73·3	63·3	0·4
2 0 2	59·4	67·5	0·6	24·2	23·4	0·4
2 1 2	192·2	198·9	0·6	55·2	72·2	0·4
0 0 4	27·5	37·2	0·5	6·4	18·1	0·4
2 2 0						
1 3 1	53·3	36·3	1·2			
0 1 4	315·2	315·2	1·2	135·6	119·4	0·5
1 2 3						
0 3 2						
2 2 2	69·2	90·0	1·0	20·6	24·2	0·6
0 2 4	75·1	113·9	3·5			
3 0 1	92·6	116·6	3·5			
0 4 0	29·5	45·0	3·2			
3 1 1	48·2	52·7	3·2			
1 3 3	6·3	8·3	3·1			
2 0 4	6·3	4·9	3·1			
2 1 4	154·1	172·9	3·4			
2 3 2						
1 0 5						
1 4 1						
0 4 2	3·4	25·0	3·1			
1 1 5	49·7	51·4	3·1			
3 2 1	32·3	23·4	3·1			

Table 3. *Fractional positional and thermal parameters with estimated standard deviations from the least-squares refinements*

The tabulated thermal parameters are related to the temperature factor by the expression†

$$\exp[-\tfrac{1}{4}(B_{11}h^2a^{*2} + B_{22}k^2b^{*2} + B_{33}l^2c^{*2} + 2B_{12}hka^*b^* + 2B_{13}hla^*c^* + 2B_{23}klb^*c^*)].$$

	Parameter	DF 4·2 K	DF 85 K	HF‡ 148 K
F	x	0·0	0·0	0·0
	y	0·25	0·25	0·25
	z	0·126 (2)	0·125 (4)	0·115
	B (Å^2)	0·6 (4)	0·9 (7)	
	B_{11} (Å^2)	0·3 (5)		3·8
	B_{22} (Å^2)	0·2 (13)		1·3
	B_{33} (Å^2)	0·7 (10)		3·8
D	x	0·0	0·0	0·0
	y	0·444 (5)	0·430 (8)	
	z	0·036 (3)	0·025 (6)	
	B (Å^2)	1·7 (4)	3·1 (10)	
	B_{11} (Å^2)	1·8 (9)		
	B_{22} (Å^2)	1·2 (11)		
	B_{33} (Å^2)	2·7§		
	B_{23} (Å^2)	1·1§		
	$\langle\varphi_{in}^2\rangle^{1/2}$(°)	11 (16)		
	$\langle\varphi_{out}^2\rangle^{1/2}$(°)	8 (7)		
	r(F–F) (Å)	2·50 (1)	2·51 (2)	2·49 (1)
	r(F–D) (Å)	0·95 (2)	0·93 (3)	
	r(F–D)$_{cor}$ (Å)	0·97 (2)	0·95 (3)	
	∠(F–F–F) (°)	116·6 (10)	116·7 (15)	120·1

† $\beta_{11} = B_{11}a^{*2}/4 = 2\pi^2 a^{*2} T_{11}$.
‡ Values obtained by Atoji & Lipscomb (1954)
§ Thermal parameters which were linked to others in the least-squares refinement.

Least-squares refinements

(*A*) *Isotropic*

The least-squares refinements of the structural parameters were performed with a modified version of *ORFLS* (Busing, Martin & Levy, 1962). The modification was necessary in order to obtain a least-squares fit to the intensities of multiplet as well as single peaks. (It will be seen from Table 2 that the 4·2 K data contained four and the 85 K data two unresolvable multiplets.) In these refinements the measured intensities were weighted by $1/\sigma_d^2(hkl)$. The values of $I_d(hkl)$, $\sigma_d(hkl)$ and $I(hkl)_{calc}$, obtained after five cycles, are listed in Table 2. It should be noted that the $I_d(hkl)$ are observed intensities, uncorrected for Lorentz factor or multiplicity, the $I(hkl)_{calc}$ being calculated accordingly. The positional and thermal parameters of the deuterium and fluorine atoms obtained from the isotropic refinements are summarized in Table 3.

(*B*) *Anisotropic*

The data collected at 4·2 K were more extensive than those at 85 K, and it was thought they may be adequate to evaluate the anisotropy in the thermal motion of the atoms, and to compare it with that expected from the zero-point motion of the molecule.

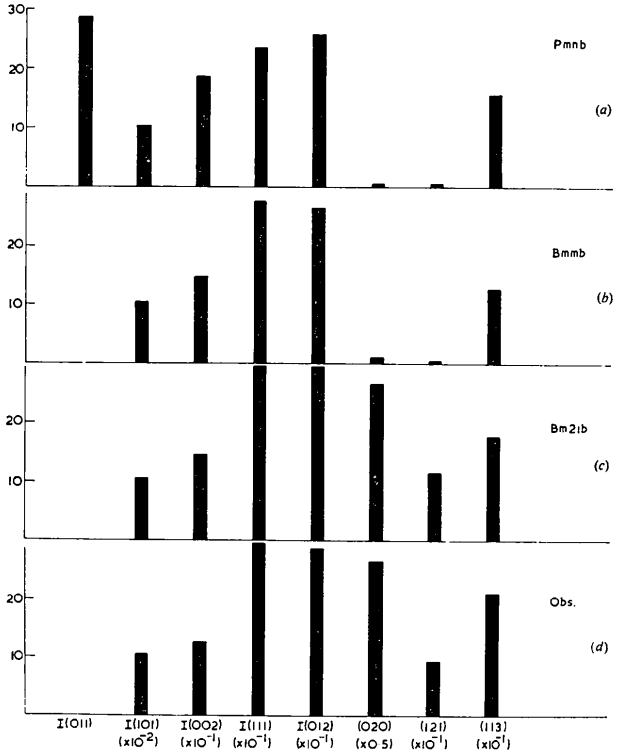

Fig. 2. Comparison of the intensities of the first few powder peaks of solid DF observed at 4·2 K (*d*) with calculated intensities based on the antiparallel zigzag chain model (*a*), the disordered zigzag chain model (*b*) and the parallel zigzag chain model (*c*).

Since the motions of individuals atoms are of less interest than the 'rigid body' translational and angular vibrations of the molecules, the following quantities were sought from the refinement: T_{11}, T_{22}, T_{33} – the diagonal components of the translational vibration tensor, $\langle\varphi_{in}^2\rangle$ – the mean square amplitude of molecular libration about [100], $\langle\varphi_{out}^2\rangle$ – the mean square amplitude of molecular libration about an axis in the (100) plane perpendicular to the molecular axis.

Following the method of Cruickshank (1956*a*) for a rigid molecule we obtain, for the F atom:

$$\beta_{ii}=2\pi^2 a_i^{*2}T_{ii} \tag{4}$$

where $a_1^*=a^*$, $a_2^*=b^*$, $a_3^*=c^*$; and β_{ij} are the quantities appearing in the anisotropic temperature factor $\exp[-(h^2\beta_{11}+k^2\beta_{22}+\ldots 2hk\beta_{12}+\ldots)]$. Similarly for the D atom

$$\beta_{11}=2\pi^2 a^{*2}[T_{11}+L^2\langle\varphi_{out}^2\rangle] \tag{5}$$

$$\beta_{22}=2\pi^2 b^{*2}[T_{22}+z^2\langle\varphi_{in}^2\rangle+\langle u_s^2(\mathrm{D})\rangle_{22}] \tag{6}$$

$$\beta_{33}=2\pi^2 c^{*2}[T_{33}+y^2\langle\varphi_{in}^2\rangle+\langle u_s^2(\mathrm{D})\rangle_{33}] \tag{7}$$

$$\beta_{23}=2\pi^2 b^*c^*[-yz\langle\varphi_{in}^2\rangle+\langle u_s^2(\mathrm{D})\rangle_{23}]\,. \tag{8}$$

The terms $\langle u_s^2(\mathrm{D})\rangle_{ij}$ in equations (6)–(8) are contributions from the stretching mode of the molecule. These were calculated from the total zero-point stretching amplitude $\langle u_s^2(\mathrm{D})\rangle$ using the relationship

$$\langle u_s^2(\mathrm{D})\rangle_{ij}=\langle u_s^2(\mathrm{D})\rangle(\mathbf{L}\,.\,\mathbf{a}_i)(\mathbf{L}\,.\,\mathbf{a}_j)/|\mathbf{L}|^2|\mathbf{a}_i|\,|\mathbf{a}_j| \tag{9}$$

(where **L** is the molecular axis and $\mathbf{a}_1=\mathbf{a}$, $\mathbf{a}_2=\mathbf{b}$, $\mathbf{a}_3=\mathbf{c}$). $\langle u_s^2(\mathrm{D})\rangle$ was calculated by taking the stretching frequency to be the mean ($=2600\ \mathrm{cm}^{-1}$) of the two infrared stretching frequencies for DF measured by Kittelberger & Hornig (1967) and assuming the stretching motion to be harmonic and in its ground state.

With $\langle U_s^2(\mathrm{D})\rangle$ assumed to be known, equations (4)–(8) were used to express β_{22}^{D} and β_{23}^{D} in terms of β_{33}^{D} and β_{33}^{F}. Accordingly, out of the seven non-zero anisotropic thermal parameters, only five (β_{11}^{F},β_{22}^{F},β_{33}^{F}, β_{11}^{D},β_{33}^{D}) were allowed to vary in the least-squares refinement; the remaining two (β_{22}^{D} and β_{23}^{D}) were constrained to conform with equations (6), (7), (8). The results of this refinement are shown in Table 3.

Assuming that (i) at 4·2 K the molecules are predominantly in their ground state, and (ii) that the translational and angular vibrations of the molecules are harmonic, the expected values of $\langle\varphi_{in}^2\rangle$, $\langle\varphi_{out}^2\rangle$, T_{11}, T_{22} and T_{33} can be calculated from the assigned infrared and Raman frequencies.

The frequencies and amplitudes of the zero-point motion obtained this way from the spectroscopic data are summarized in Table 4, together with the amplitudes calculated from the neutron-diffraction least-squares refinements.

Because of the large angular librations of the molecules, the F–D bond length calculated from the positional parameters of the atoms appears to be shorter than its true value (Cruickshank, 1956*b*). A useful

Table 4. *Comparison of root mean square vibrational amplitudes of the* DF *molecules at* 4·2 K *calculated from spectroscopic and neutron-diffraction data*

Mode	Root mean square amplitudes of zero-point motion	Root mean square amplitudes from neutron diffraction	ν(cm^{-1}) (Kittelberger & Hornig, 1967)
$\langle\varphi_{in}^2\rangle^{1/2}$	6·5°	11 (16)°	699
$\langle\varphi_{out}^2\rangle^{1/2}$	8·6°	8 (7)°	401
$(T_{11})^{1/2}$	0·06 Å	0·06 (8) Å	210
$(T_{22})^{1/2}$	0·047 Å	0·05 (13) Å	360
$(T_{33})^{1/2}$	0·06 Å	0·09 (12) Å	210

expression for estimating this apparent bond-length shortening is given by Busing & Levy (1964):

$$\Delta L = \frac{L}{2} \sum_{i=1}^{n} \langle\varphi_i^2\rangle \sin^2 \psi_i$$

where L is the apparent bond length calculated from the positional parameters of the atoms, ΔL the correction to the apparent bond length, $\langle\varphi_i^2\rangle$ the mean square amplitude of libration about the ith axis and ψ_i the angle between the ith librational axis and the molecular axis. The values of the corrected F–D bond length obtained this way at 4·2 and 85 K are given in Table 3.

Discussion

The present investigation established that the hydrogen-bonded molecules in solid DF form parallel rather than antiparallel zigzag chains and there is no disorder in the deuterium positions. The crystal structure of DF is shown schematically in Fig. 1(*a*). The orthorhombic unit cell has the following dimensions: $a=3{\cdot}31(1)$, $b=4{\cdot}26(1)$, $c=5{\cdot}22(1)$ Å at 4·2 K and $a=3{\cdot}33(1)$, $b=4{\cdot}27(1)$, $c=5{\cdot}27(1)$ Å at 85 K. The space group is $Bm2_1b$ with four molecules in the unit cell. The calculated density is $\varrho=1{\cdot}89$ g cm^{-3} at 4·2 K and $\varrho=1{\cdot}86$ g cm^{-3} at 85 K.

The 2% increase in volume between 4·2 K and 85 K is mainly due to the increase of the c parameter of the unit cell; the a and b parameters hardly change at all. The F–F distances and F–F–F angles of neighbouring fluorine atoms also remain practically constant between 4·2 K and 85 K (see Table 4), indicating the rigidity of the fluorine skeleton. In contrast to this, the orientation of the molecular axis relative to the chain axis varies significantly with the temperature. At 4·2 K the angle between the axis of a DF molecule and the chain axis DF$\wedge b=29{\cdot}6°$, while at 85 K it increases to 34·4°. At the same time the angle between the F–F direction and the chain axis remains constant within the experimental error (31·6° at 4·2 K and 31·7° at 85 K). Hence the axis of the DF molecule rotates through nearly 5° within the practically unchanged fluorine frame while the temperature rises from 4·2 K to 85 K. Similar behaviour was observed earlier in the ordered low phase of solid DCl which has a similar hydrogen-bonded parallel zigzag chain structure (Farrow, 1970).

The parallel zigzag chain structure proposed for DF is compatible with the results of the spectroscopic studies quoted in the *Introduction*. In particular, such a structure is expected to exhibit two coincident infrared and Raman stretching frequencies, in agreement with the observations of Kittelberger & Hornig (1967). Furthermore, the significantly longer F–D bond as compared with the gas-phase value of 0·92 Å and its increase with decreasing temperature (see Table 4) agree with the conclusions drawn by Habuda & Gagarinsky (1971, 1972) from their n.m.r. experiments. The observed bond-length increase is also compatible with the results of Kittelberger & Hornig (1967) who found that the stretching frequency decreased with decreasing temperature.

Though the crystal structure proposed for DF on the basis of our neutron powder-diffraction studies contradicts three previous suggestions made for the structure of solid HF (see *Introduction*), nevertheless, solid HF is expected to be isomorphous with the parallel-chain structure described above for the following reasons:

(i) The two compounds are isoelectronic.

(ii) The infrared and Raman studies of Kittelberger & Hornig (1967) show a close correlation between the absorption spectra of solid HF and DF.

(iii) The shapes and dimensions of the unit cells of solid HF and DF are very similar. Though the diffraction studies of solid HF and DF were carried out at different temperatures, the ratios of the corresponding lattice parameters are very nearly equal: $a_{HF}/a_{DF}=1{\cdot}02_7$, $b_{HF}/b_{DF}=1{\cdot}01_2$, $c_{HF}/c_{DF}=1{\cdot}02_7$.

Although these arguments do not constitute conclusive evidence for isomorphism, we believe this to be the most reasonable assumption, given the experimental evidence available at present.

We thank D. H. C. Harris and the staff of the Dido and Pluto reactors for supporting the neutron diffraction work at Harwell, and Colin Hotston and Peter Cruze at Queen Mary College for technical assistance. We also thank the Science Research Council, the Neutron Beam Research Committee and the Iranian Government for financial support.

References

ATOJI, M. & LIPSCOMB, W. N. (1954). *Acta Cryst.* **7**, 173–175.

BACON, J. & SANTRY, D. P. (1972). *J. Chem. Phys.* **56**, 2011–2016.

BAUER, S. H., BEACH, J. Y. & SIMONS, J. H. (1939). *J. Amer. Chem. Soc.* **61**, 19–24.

BOUTIN, H., SAFFORD, G. J. & BRAJOVIC, V. (1963). *J. Chem. Phys.* **39**, 3135–3140.

BRIEGLEB, G. (1941). *Z. Phys. Chem.* **B51**, 9–38.

BRIEGLEB, G. (1942). *Z. Phys. Chem.* **B52**, 368.

BRIEGLEB, G. (1943). *Z. Phys. Chem.* **B53**, 225–226.

BUSING, W. R. & LEVY, H. A. (1964). *Acta Cryst.* **17**, 142–146.
BUSING, W. R., MARTIN, K. O. & LEVY, H. A. (1962). *ORFLS*. Oak Ridge National Laboratory Report ORNL-TM-305.
CLUSIUS, K., HILLER, K. & VAUGHAN, J. V. (1930). *Z. Phys. Chem.* B**8**, 427–439.
CRUICKSHANK, D. W. J. (1956*a*). *Acta Cryst.* **9**, 754–756.
CRUICKSHANK, D. W. J. (1956*b*). *Acta Cryst.* **9**, 757–758.
DAHMLOS, J. & JUNG, G. (1933). *Z. Phys. Chem.* B**21**, 317–322.
FARROW, R. F. C. (1970). Ph. D. Thesis, London.
GIGUÈRE, P. A. & ZENGIN, N. (1958). *Canad. J. Chem.* **36**, 1013–1019.
GÜNTHER, P., HOLM, K. & STRUNZ, H. (1939). *Z. Phys. Chem.* B**43**, 229–239.
HABUDA, S. P. & GAGARINSKY, YU. V. (1971). *Acta Cryst.* B**27**, 1677–1678.
HABUDA, S. P. & GAGARINSKY, YU. V. (1972). *Sov. Phys.* **17**, 80–81.
HERBER, R. H. (1962). *Inorganic Isotopic Syntheses*. New York: W. A. Benjamin.
HU, J. H., WHITE, D. & JOHNSTON, H. L. (1953). *J. Amer. Chem. Soc.* **75**, 1232–1236.
KITTELBERGER, J. S. & HORNIG, D. F. (1967). *J. Chem. Phys.* **46**, 3099–3108.
RING, J. W. & EGELSTAFF, P. A. (1969). *J. Chem. Phys.* **51**, 762–770.
RING, J. W. & EGELSTAFF, P. A. (1970). *J. Chem. Phys.* **52**, 5973–5974.
SASTRI, M. L. N. & HORNIG, D. F. (1963). *J. Chem. Phys.* **39**, 3497–3502.
SMITH, D. F. (1958). *J. Chem. Phys.* **28**, 1040–1056.

Acta Cryst. (1975). B**31**, 2003

The Crystal Structure of Bismuth Thiophosphate $BiPS_4$

BY H. ZIMMERMANN, C. D. CARPENTIER AND R. NITSCHE

Kristallographisches Institut der Universität, D-78 Freiburg i. Br., Hebelstr. 25, Germany (BRD)

(*Received* 18 *February* 1975; *accepted* 20 *February* 1975)

Crystals of $BiPS_4$ have been grown from the vapour phase by iodine transport. They are orthorhombic, space group *Ibca*, $a=10{\cdot}601$ (2), $b=11{\cdot}112$ (3), $c=19{\cdot}661$ (4) Å; $Z=16$. The intensities were measured on a Nonius CAD-4 diffractometer. A Patterson synthesis revealed the basic structure. A least-squares refinement with anisotropic temperature factors for Bi and P led to a final R of 0·047. The structure consists of a network of S tetrahedra, every second of which is occupied by a P atom. Alternating chains of edge-shared tetrahedra, running parallel to **a** and **b** are stacked along **c**. Six- and eightfold coordination of S around Bi occurs.

Introduction

Synthesis and crystal growth (by vapour transport with iodine between 590 and 560 °C) of $BiPS_4$ has been reported (Nitsche & Wild, 1970). The structures of BPS_4 and $AlPS_4$ have been solved by Weiss & Schaefer (1963, 1960). The structure of $InPS_4$ has been determined by Carpentier, Diehl & Nitsche (1970), that of $GaPS_4$ by Buck & Carpentier (1973). Since all these structures are different, a structure determination of $BiPS_4$ seemed appropriate to gain further insight into the crystal chemistry of thiophosphates.

Experimental

Crystal data

Vapour-grown $BiPS_4$ crystals are rhombic prisms, elongated along [110]. They have a metallic, gray lustre; the powder is dark red. Observations on very thin platelets in polarized light showed the crystals to be twinned along (110). The formula was confirmed by chemical analysis. F. W. 368·24. Lattice parameters (20 °C): $a=10{\cdot}601$ (2), $b=11{\cdot}112$ (3), $c=19{\cdot}661$ (4) Å, $V=2309{\cdot}1$ (1) Å^3, $Z=16$, $D_m=4{\cdot}18$, $D_c=4{\cdot}22$ gcm^{-3}. Reflexion conditions: hkl: $h+k+l=2n$, $0kl$: $k=2n$, $h0l$: $l=2n$, $hk0$: $h=2n$. Space group: *Ibca*. Mo $K\alpha$, $\lambda=0{\cdot}7109$ Å; μ (Mo $K\alpha$) = 306 cm^{-1}. Crystal size: 0·04 × 0·05 × 0·07 mm.

The cell parameters were obtained by a least-squares refinement of Guinier powder data (Cu $K\alpha_1$, $\lambda=1{\cdot}54051$ Å) with the X-RAY 70 System (*PARAM*; Stewart, Kundell & Baldwin, 1970).

Data collection

Numerous crystals were checked on a precession camera but no untwinned specimens could be found or prepared. Finally a crystal with dimensions 0·04 × 0·05 × 0·07 mm containing 70% and 30% of the twins was selected. The two lattices transform into each other by reflexion across (110). The crystal was set with **c** parallel to the axis of the goniometer. The intensities were collected on a computer-controlled four-circle diffractometer (Nonius CAD-4) with Mo $K\alpha$ radiation from a graphite monochromator. The intensities were measured with a scintillation counter.

The ω–2θ scan method was used for a quarter of the